

# Simulation of Light Interaction with Metallic Nanoparticles

Saulius Juodkazis\*, Hiroaki Misawa\*, Egidijus Vanagas\*\*, and Mingwei Li\*\*\*

\*CREST-JST & RIES, Hokkaido University, Sapporo 001-0021, Japan

E-mail: Misawa@es.hokudai.ac.jp; Saulius@es.hokudai.ac.jp

\*\* Laser Systems Inc., NRK Bldg., N15-W4, Sapporo 001-0015, Japan

\*\*\* Spectra-Physics, Newport Corporation, 1330 Terra Bella Avenue, Mountain View, CA 94043, USA

A high-precision 3D structuring of dielectrics by sub-1 ps pulses is possible by dielectric breakdown and opens a unique possibility to create a high temperature electrons inside material under processing. The 3D nano/micro-structuring by dielectric breakdown is numerically simulated by 3D finite-differences time domain (FDTD) calculations where the plasma is simulated by a nano-sphere of metal (gold). The effect of anisotropic light scattering in the plane of incident polarization has been qualitatively explained by light interaction with ionized (metallic) focal volume. It is shown that the experimentally achieved densification of materials after irradiation by tightly focused sub-1 ps pulses is consistent with formation of new high-pressure phases.

**Keywords:** Laser microfabrication, heat affected zone, thermal effects, laser breakdown, shock effects

## 1. Introduction

Three-dimensional (3D) laser micro-fabrication [1,2,3,4,5] approaches the 100 nm benchmark of nanofabrication in two different ways: (i) laser radiation tightly focused into a spot size comparable with the wavelength can induce photo-modification considerably smaller than 100 nm [6,7], and, also, (ii) the photo-modified new phases of materials with altered structural and chemical properties can be found inside the focal spot of laser irradiated region in the form of nano-structured materials with feature sizes smaller than 100 nm [8]. New nano-materials can be created at the focus region where transient high pressure is created by a shock wave. Thermal effects are apparently reduced when laser radiation with shorter pulse durations are employed in a 3D or surface (by ablation) structuring of materials, since the heat diffusion during irradiation become less important mechanism of energy delivery resulting in a reduced heat affected zone (HAZ).

In the case of ultra-short (sub-1 ps) pulses, the temperature of electrons can be much higher than that of ions(atoms) and is equilibrated mainly by the fastest Auger recombination, which rate is strongly dependent on the densities of electron,  $N_e$ , and ions,  $N_i$ , as  $(N_e^2/N_i)$  [12]. Hence, laser radiation provides the way to deliver and localize in a small volume the high temperature source. Also, the high energy (10 - 100 eV) electrons become a EM-radiation source at visible, UV, and X-rays regions via bipolar recombination and Bremsstrahlung. Re-absorption of those short wavelength radiations occurs at the nearest proximity of the ionized focus. This makes an unique opportunity to create a strongly absorbed light source from the inside and can this be realized by ultra-short pulses. This is a prospective method for photo-structuring of materials at high sub-wavelength resolution and can be used in photo-polymerization of resists and resins as well as in photo-modification of photo-sensitive glasses. Hence, the ionization of the irradiated volume is a key process to un-

derstand thermal and structural effects upon irradiation by ultra-short pulses. Also, the spatial extent of the ionized volume is a critical parameter defining the size of final photo-modification.

Here, we model the light-plasma interaction by placing a nano-sphere of a metal (a plasma material) into a plane wave. Spectral and spatial effects of light scattering by such a plasma nano-sphere are revealed by a 3D finite differences time domain (FDTD) calculations. The "propeller effect" [9] of anisotropic light scattering in the plane of incident polarization will be qualitatively explained by a light scattering on the breakdown plasma. The breakdown generated pressure will be compared with predictions based on equation of state (EOS) showing that the pressures large enough for new phase generation can be reached.

## 2. Model

We consider here a tight focusing geometry when ultra-short laser radiation is focused inside dielectric materials: crystals, glasses, and polymers and produces a dielectric breakdown (an ionization of the focal volume) which causes a micro-explosion due to high pressure generated by a strong absorption in a skin-depth of the ionized focal volume [10,14]. The focal spot is typically smaller than wavelength of laser radiation (800 nm in this case) when focusing is carried out with a high numerical aperture  $NA > 1$  objective lens. Since by a dielectric breakdown a plasma is produced at the focus, which can be modeled as a perfect metal (a Drude model of dielectric function), the light interaction with a nano-sphere of metal can be used as a model for qualitative analysis of the light-matter interaction. Structural modifications including a void formation can be localized within the volume about one micrometer in cross-section in all considered dielectric materials. In the case of single pulse irradiation, the photomodification results from self-action of the pulse, i.e., the ionization at the pulse front affects propagation of its trailing part.

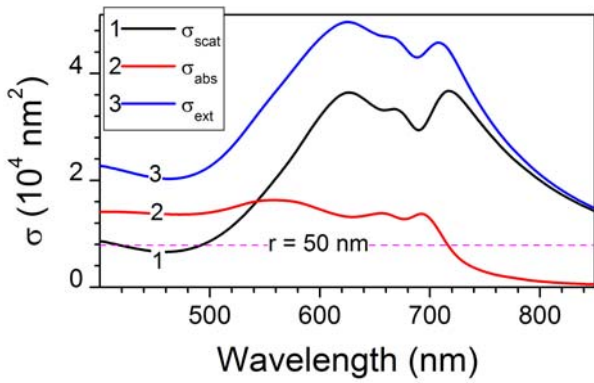


**Fig. 1** Spectra of the absorption, scattering, and extinction cross-sections of a 50-nm-radius gold nanosphere inside dielectric of refractive index  $n = 1.7$ . Calculated by 3D-FDTD program FDTD Solutions *Lumerical*.

**3. Dielectric breakdown**

The dielectric breakdown or an ionization of the focal volume inside transparent dielectric (PMMA, silica glass, quartz, sapphire, etc.) creates a plasma which has an absorbance of  $\sim 0.6$  at full ionization of the dielectric [11]. The breakdown is driven mainly by avalanche because it is most efficient at a high solid-state density generated with typical intensities of  $1\text{-}100\text{ TW/cm}^2$ . This is in contrast to the breakdown in gas, where an incoming light-field is screened by the ionized plasma. The avalanche, though probable inside the field's penetration region, is not effective

because of low gas density. In solid state material, the avalanche becomes a dominant mechanism, even when a nonlinear multi-photon ionization initially ionizes the focal volume, since the atom density in a skin-depth (the extent of evanescent field penetration) can be very high [12].

The full ionization of the focal volume occurs in few optical cycles at irradiance of about  $10^{14}\text{ W/cm}^2$  typical for the most laser microstructuring experiments. The initial electrons are created by multi-photon absorption in dielectric. A multiply-ionized plasma of high temperature is created during the ultra-short laser radiation. The localization of absorption in such plasma is within the absorption volume defined by a skin-depth of  $50\text{--}70\text{ nm}$  (at conditions of interest for nano-/micro-fabrication). Hence, a volume which dimensions are tens-of-nm becomes a multiply ionized plasma, where temperature of electrons is much higher than that of ions. This condition last approximately as long as the pulse, since the duration of Auger recombination is just tens-of-fs at electron-ion densities comparable to those of solid state material  $\sim 10^{22}\text{ cm}^{-3}$ . After the optical pulse, a high pressure region causes a microexplosion with a out-bound shock wave while a rarefaction wave simultaneously is formed and propagates in-bound in accordance to mass conservation [12].

**4. FDTD simulation of breakdown**

Three-dimensional FDTD calculations were carried out to simulate the interaction between the ionized focal volume (plasma) with the incoming laser pulse using the soft-

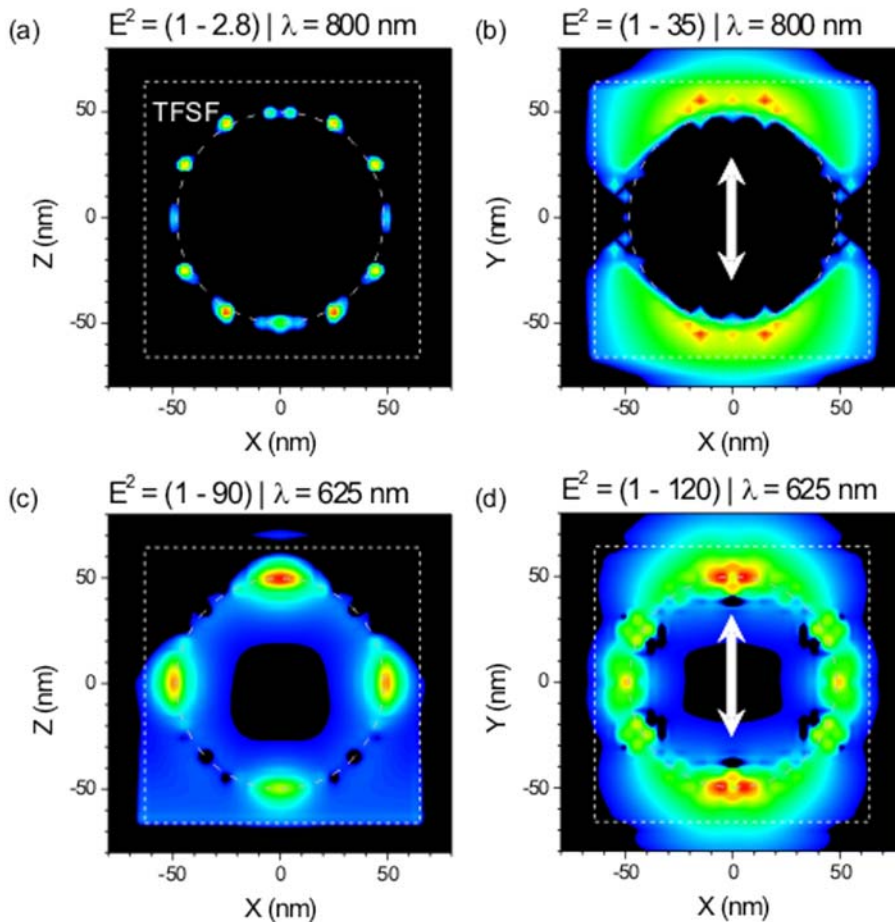


**Fig. 2** 3D-FDTD simulations of spatial intensity distributions of a plane wave  $E(0,1,0)$  interaction with a 50-nm-radius gold sphere (the outline is marked) in dielectric of refractive index  $n = 1.7$ . Light propagation is along z-axis. TSFT designates the total-field scattered-field light source in *Lumerical* program and is marked by dashed square. Intensity  $E_y^2$  maps at 800 and 625 nm are plotted in logarithmic scale in (a,b) and (c,d), respectively.

ware package FDTD Solutions (*Lumerical Solutions, Inc.*) [13]. The FDTD simulates propagation of light by solving Maxwell equations numerically, i.e., by propagating light from the modeled light source through the complex structures using a user-defined spatial grid. Spatial discretization of 5 nm was used in all calculations and was adequate for qualitative discussions of light scattering on a 50-nm-radius sphere. The metallic breakdown plasma was modeled by placing a gold nano-sphere of 50 nm radius at the focus. The size corresponds approximately to the absorption skin-depth in metals. It has been confirmed experimentally that the micro-explosion starts from a comparable focal volume [14]. The choice of gold was justified by the high electron density  $5.9 \times 10^{22} \text{ cm}^{-3}$  and good compliance of its electronic response with that of an ideal metal, which dielectric function can be modeled by the Drude approximation. It should be mentioned, that particular features of extinction spectrum are determined by the gold dielectric function implemented in *Lumerical* (the dielectric function from ref. [15] was used).

The total-field scattered field (TFSF) light source was defined for simulations with FDTD *Lumerical* software. The TFSF source determines the inter-volume around the nano-object where the incident and scattered fields are present (the total field region) and the outside volume where only the scattered field is calculated. It allows one to calculate spectral cross-sections of absorption and scattering when the dielectric function of the nano-object is provided (a gold particle in our case). The TFSF source is only defined as a plane wave in the used software, hence, there was no possibility to model tight focusing used in real experiments. However, in the waist region of tightly focused laser radiation, the plane wave approximation is qualitatively adequate because the light passes throughout the focal region which length is the double Rayleigh length (3-4  $\mu\text{m}$  in our case) as a plane wave.

Figure 1 shows the 3D-FDTD simulated spectra of absorption, scattering, and extinction cross-sections (where  $\sigma_{\text{ext}} = \sigma_{\text{abs}} + \sigma_{\text{scat}}$ ) of a gold nano-sphere. The maximum values of scattering cross-section are much larger than a geometrical cross-section given by a dashed line in Fig. 1 (i.e., light “sees” a larger particle as compared with its geometrical dimensions). The particular spectral shape shown in Fig. 1 is due to an excitation of plasmon in the metallic particle and is determined with the experimentally measured dielectric function of gold used in FDTD software. Hence, the spectral features such as local maxima and minima in the extinction spectra (Fig. 1) are size-dependent.

The spatial intensity distribution is shown in Fig. 2, where the enhancement of intensity  $E_y^2 > 1$  is plotted, i.e., the light intensity of the same polarization as that of the incident pulse is mapped in different cross-sections and at two different wavelengths (the incident field is  $E_y = 1$ ) as shown in (a,b) and (c,d) panels, respectively. The cross-sections are taken through the center of the nano-sphere. The presence of plasmonic excitation on the surface of the gold nano-sphere is manifested by an intensity distribution which shows 3D localization points (see, a high intensity regions in Fig. 2). The locations of the high intensity are dependent on the wavelength, however, such regions are all the time present on the poles (along the polarization direc-

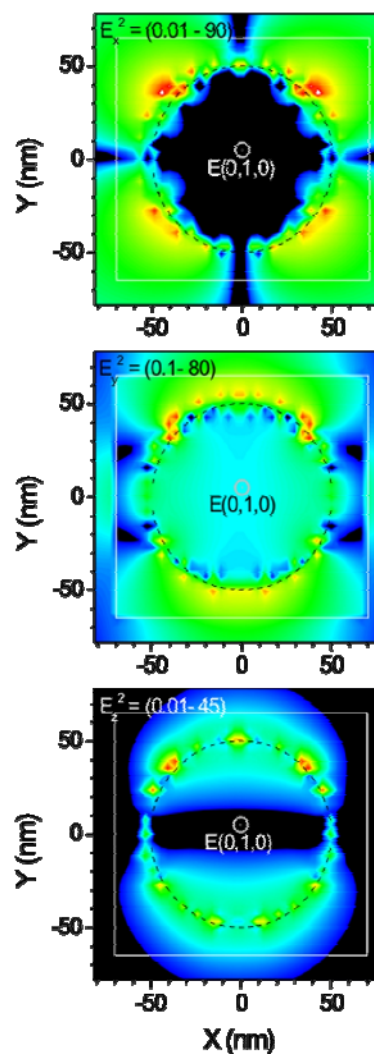


**Fig. 3** FDTD spatial intensity distribution of different components (simulation conditions are the same as in Fig. 2). The vertical position of the light source was at +0.5 nm (instead of 0 nm due to this particular discretization), hence, an unsymmetrical light intensity distribution resulted in the calculated field distributions, the intensity was slightly larger for positive y-values. The wavelength of light was 720 nm.

tion) as can be seen in (a,b) and (c,d) panels. In the case of real experiments with ionization and breakdown of dielectrics, there are no sharp boundary between the ionized (metallic) and dielectric regions, however the qualitative features of light scattering by a plasma volume are expected to be similar.

In particular, a “propeller effect”, the anisotropic light scattering along the polarization, which can not be explained by classical dipole emission [9] was revealed in 3D-FDTD simulations (Fig. 2(b,d)). The regions of highest light intensity  $E_y^2$ , much higher than the incident intensity are localized on the rim of nano-sphere at the poles along the direction of incident polarization. Hence, the ionization and luminescence are expected to have similar spatial distributions and have maxima along the polarization of incident light when observed in a far-field. This explains the “propeller effect” [9].

Additional corroboration of the proposed explanation is shown in Fig. 3, where all three intensity components are plotted for the incident  $E(0,1,0)$  field. All the intensity

components show spatial distributions, which have dipolic properties with the maxima along the incident polarization. Those maxima are considerably enhanced as compared to the incident intensity.

Figure 3 demonstrates that the actual light-field localization and enhancement effects as a spatial intensity distribution of the incident light. The plane wave source was 0.5 nm shifted out of center in calculations by the algorithm implemented in the used FDTD software (a more dense calculation grid would reduce this unintended shift). The result is obvious as the asymmetric features in light intensity distribution, though the qualitative result of dipolic scattering is clearly seen.

It is noteworthy, that light filamentation in water and glasses was found also strongly dependent on the spatial intensity distribution at the focus. Also, the light filamentation is caused by the light-induced absorption which transforms an initially Gaussian lateral laser intensity distribution into a Bessel-type one. Further studies of more realistic focal volumes of ionized plasma should be considered for the comparison with the actual filamentation patterns.

The temporal evolution of the breakdown is not well known because it occurs within several optical cycles at high irradiance (tight-focusing) and appears as instantaneous in the most experiments [16]. As 3D-FDTD simulations show (Fig. 1) the scattering is spectrally dependent on the size of the ionized plasma region (a diameter of the metal sphere). For, example, a larger 80-100 nm radius nano-sphere would have a stronger scattering at the larger 800 nm wavelength, the actual wavelength of irradiation in the most of experiments (this was tested by numerical simulations). One can expect that the breakdown is more plausible due to such enhancement. The larger extinction means that the nano-particle is excited and re-emits that particular wavelength. Hence, the ionized volume and the scattering enhancement are expected to be inter-connected in a self-consistent manner (the FDTD procedure did not simulate the ionization).

Concluding, the ionization of focal volume explains the “propeller effect”. The model of cw-plane wave passing the nano-particle can only serve as a qualitative model, since the pulsed irradiation corresponds to reality. It is noteworthy, that the light passes the focus as a plane wave even at tight focusing making the used model qualitatively adequate. Since the breakdown ionization leads to the shock-wave generation from the ionized volume of tens-of-nanometers in dimensions, we considered next the pressures which are created inside the shock-affected volume.

### 5. Shock-compressed region

The laser pulse focused inside sapphire, quartz, or glass typically creates a void surrounded by a densified material (in the case of crystalline dielectrics it is amorphous) at pulse energies lower than the onset of crack formation [17]. The void is formed as a result of rarefaction wave, while the out-bound shock wave causes densification. The densification up to 12-15% is reached in a densified shell around the void as followed from mass conservation. The Birch equation of state fitting the pressure-volume data of the various phases is given by [18]:

$$P/B_0 = \frac{3}{2}(x^{7/3} - x^{5/3}) \left[ 1 + \frac{3}{4}(B_0' - 4)(x^{2/3} - 1) \right], \quad (1)$$

where the relative volume change is  $x=V_0/V$  ( $V_0$  is the zero-pressure volume and  $V$  is the volume at pressure  $P$ ),  $B_0$  and  $B_0'$  are the isothermal bulk modulus and its derivative at zero pressure, respectively. For example, in the case of the rutile phase of  $\text{TiO}_2$  ( $B_0 = 230$  GPa,  $B_0' = 6.6$ ) [18]. A similar low compressibility phase is also common in silica as the stishovite at high pressure. The compaction of  $x = 1.12 - 1.15$  would correspond to a pressure of  $P = 38 - 50$  GPa (calculated by eqn. 1). Such pressures are already few times higher than those at which phase transitions occur. The shock-compressed regions can have different phases of materials. Since temperature rise and fall are very rapid as the shock wave propagates through the surrounding volume, the high pressure phases should be present in a metastable form, so called, recoverable to the normal conditions (room pressure and temperature) [19].

### 7. Conclusions

Dielectric breakdown has been simulated by the interaction of laser radiation with a metallic (gold) nano-sphere using 3D-FDTD algorithm. The “propeller effect” has been qualitatively explained. Hence, the ionization of the focal spot accounts for the anomalous light scattering observed earlier [9]. It is also demonstrated that pressures high enough for generation of new phases are feasible in a shock-compressed crystalline materials.

### Acknowledgments

We gratefully acknowledge discussions with Prof. E. G. Gamaly on the dielectric breakdown and with Dr. V. Mizeikis on FDTD modeling.

### References

- [1] K. Sugioka, Y. Cheng, K. Midorikawa, F. Takase, and H. Takai: *Opt. Lett.*, 31, (2006) 208.
- [2] W. Watanabe, Y. Note, and K. Itoh: *Opt. Lett.*, 30, (2005) 2888.
- [3] K.-I. Kawamura, M. Hirano, T. Kurobori, D. Takamizu, T. Kamiya, and H. Hosono: *Appl. Phys. Lett.*, 84, (2004) 311.
- [4] N. Takeshima, Y. Narita, T. Nagata, S. Tanaka, and K. Hirao: *Opt. Lett.*, 30, (2005) 537.
- [5] K. Shirota, H. Sun, and S. Kawata: *Appl. Phys. Lett.*, 84, (2004) 1632.
- [6] S. Juodkazis, V. Mizeikis, K. K. Seet, M. Miwa, and H. Misawa: *Nanotechnology*, 16, (2005) 846.
- [7] T. Kondo, S. Juodkazis, and H. Misawa: *Appl. Phys. A*, 81, (2005) 1583.
- [8] S. Juodkazis, K. Nishimura, H. Misawa, T. Ebisui, R. Waki, S. Matsuo, and T. Okada: *Adv. Mat.* (2006) in press DOI: 10.1002/adma.200501837
- [9] P. G. Kazansky, H. Inouye, T. Mitsuyu, K. Miura, J. Qiu, K. Hirao, and F. Starrost: *Phys. Rev. Lett.*, 82, (1999) 2199.
- [10] E. N. Glezer, M. Milosavljevic, L. Huang, R. J. Finlay, T.-H. Her, J. P. Callan, and E. Mazur: *Opt. Lett.*, 21, (1996) 2023.

- 
- [11] E. G. Gamaly, A. V. Rode, B. Luther-Davies, and V. T. Tikhonchuk: *Phys. Plasmas*, 9, (2002) 949.
- [12] E. G. Gamaly, S. Juodkazis, K. Nishimura, H. Misawa, E. G. Gamaly, B. Luther-Davies, L. Hallo, P. Nicolai, and V. T. Tikhonchuk: *Phys. Rev. B.*, 73 (2006) 214101.
- [13] A. Taflov, *Computational electromagnetics: the finite-difference time-domain method*, Artech House, Boston, (1995).
- [14] S. Juodkazis, K. Nishimura, S. Tanaka, H. Misawa, E. G. Gamaly, B. Luther-Davies, L. Hallo, P. Nicolai, and V. T. Tikhonchuk: *Phys. Rev. Lett.*, 96, (2006) 166101.
- [15] P. B. Johnson and R. W. Christy: *Phys. Rev. B*, 6 (1972) 6.
- [16] O. Efimov, S. Juodkazis, and H. Misawa: *Phys. Rev. A*, 69 (2004) 042903.
- [17] S. Matsuo, Y. Tabuchi, T. Okada, S. Juodkazis, and H. Misawa: *Appl. Phys. A*, 84, (2006) 99.
- [18] L. Gerward and J. Staun Olsen: *J. Appl. Cryst.*, 30, (1997) 259.
- [19] P. F. McMillan: *Nature materials*, 1, (2002) 19.

(Received: May 16, 2006, Accepted: December 1, 2006)